Improved Accuracy and Precision of Gas Chromatography/Mass Spectrometry Measurements for Metabolic Tracers

Bruce W. Patterson, Guohong Zhao, and Samuel Klein

The use of stable-isotope tracer methodology to study substrate metabolic kinetics requires accurate measurement of the tracer to tracee ratio (TTR), often by gas chromatography/mass spectrometry (GC/MS). Many approaches for measurement of the TTR by GC/MS do not use standards of known isotopic enrichment to control for variability in instrument response. In addition, most GC/MS applications exhibit some degree of concentration dependency whereby the measured ion abundance ratio varies with the quantity of sample analyzed, thereby placing a limitation on the accuracy of isotopic enrichment standard curves unless the quantities of standards and samples analyzed are closely matched. We document the degree to which day-to-day variability can affect the instrument response for several GC/MS analyses of metabolic tracers when isotopic enrichment standards are not used to control for variable instrument response. Furthermore, we report a new approach that incorporates concentration dependencies within a standard curve to improve the accuracy and precision of TTR measurements over a range of sample quantities analyzed. The new approach was applied to plasma samples obtained from experimental protocols performed in human subjects with three commonly used tracers: $^{2}H_2$-palmitate, $^{15}N_2$-urea, and ^{13}C-leucine. Variability in the day-to-day instrument response was 84% and 26% for $^{2}H_2$-palmitate and $^{15}N_2$-urea, respectively; in addition, up to 10% variability due to concentration dependency was noted for these applications. The new approach virtually eliminated these sources of variability. After controlling for concentration dependency, a threefold reduction in the standard error was noted when the enrichment of ^{13}C-leucine measured by electron-impact (EI) ionization GC/MS was correlated against negative chemical ionization (NCI) GC/MS. These data demonstrate that our new approach decreases the errors in TTR determination caused by variations in instrument response and concentration dependency. This approach is generically applicable, and can improve the accuracy and precision of TTR determinations for most GC/MS analyses.

STABLE ISOTOPICALLY LABELED tracers are used extensively in studies evaluating in vivo protein, fat, and carbohydrate metabolism. These studies usually involve infusion of a stable isotopically labeled tracer into the bloodstream and measurement of the subsequent tracer to tracee ratio (TTR) in blood or tissue samples. Therefore, accurate measurement of isotopic enrichment is critical for generating meaningful information regarding substrate metabolism. Stable isotopic enrichment of complex biological molecules is often measured by gas chromatography/mass spectrometry (GC/MS) because of the wide range of available derivatization reactions, GC separation media, and MS ionization modes.

Two general approaches are typically used to determine the TTR by GC/MS. The first is based on a theoretical framework that derives the TTR directly from measured ion abundance ratios using a mathematical algorithm that may use information derived either from the entire isotopomer distribution covered by the tracer and tracee[1] or from only the tracer and tracee isotopomers of interest.[2-4] This approach implicitly assumes that the ion abundance ratios measured by the instrument equate to true isotopomer ratios within the sample. Unfortunately, several processes operate within the GC/MS that invalidate this assumption. We have observed that TTR measurements for many GC/MS applications are affected by the quantity of sample analyzed. For example, the ion abundance ratio (m + 1/m + 0) of the molecular ion of methyl palmitate measured by electron-impact (EI) ionization GC/MS increases with increasing sample quantity because of a concentration-dependent, self-chemical ionization process.[5] Moreover, other processes, including isotope effects during ion fragmentation,[6] tuning conditions,[5,7,8] scatter due to concentration-dependent ion-molecule collisions,[9] detector nonlinearity,[10] and integration errors,[11] may also bias the instrument response and invalidate the assumption that measured ion abundance ratios equate to true isotopomer ratios.

The second approach to determine enrichment by GC/MS uses a calibration curve whereby measured ion abundance ratios are correlated with the enrichment of standards of known isotopic composition.[12-14] This approach corrects for many sources of measurement bias, especially variable tuning conditions. It is not practical to control all sources of instrument bias by varying the tuning conditions to ensure that measured ion abundance ratios equate to true isotopomer ratios. This is especially true when a software-based autotune rather than manual instrument tuning is used, since an autotune is designed to meet nominal instrument performance guidelines rather than the stringent requirements for absolute accuracy of ion abundance ratios. Thus, a traditional standard curve corrects for multiple measurement biases for a given instrument operating condition; however, this approach is limited by an inability to account for the concentration dependency in measured ion abundance ratios observed in most GC/MS applications.

In this report, we describe a novel approach that incorporates concentration dependencies within the framework of a standard curve to minimize TTR measurement errors by GC/MS. This approach simultaneously provides an empirical correction for multiple sources of measurement bias affecting the accuracy of ion abundance ratios (eg, tuning conditions and isotope fragmentation effects) and multiple sources of nonlinearity (eg, self-chemical ionization and ion-molecule collisions). We have

From the Division of Gastroenterology, Department of Internal Medicine, Washington University School of Medicine, St. Louis, MO.

Submitted July 21, 1997; accepted November 7, 1997.

Supported by National Institutes of Health Grants No. R01-CA62177, R01-DK49989, P41-RR00954, and RR00036.

Address reprint requests to Bruce W. Patterson, PhD, Washington University School of Medicine, 660 S Euclid Ave, Box 8127, St. Louis, MO 63110-1093.

0026-0495/98/4706-0015$03.00/0

applied this method to three commonly studied substrates: palmitate, urea, and leucine. Our results demonstrate that corrections for instrument and concentration-dependent biases can markedly improve the accuracy and precision of stable-isotope TTR measurements.

SUBJECTS AND METHODS

Human plasma samples obtained from three different study protocols were used to evaluate TTRs of different metabolic substrates. The focus of the present report is on the accuracy and precision of GC/MS enrichment measurements rather than an interpretation of substrate metabolic kinetics. All subjects provided informed consent before participating in the tracer infusion protocols, which were performed within the General Clinical Research Center (GCRC) and approved by the Human Studies and GCRC Scientific Review Committees of Washington University School of Medicine.

$^2H_2$-Palmitate

An adult male subject fasted overnight (12 hours). A catheter was placed in an antecubital vein of one arm to infuse 2,2-[$^2H_2$]-hexadecanoic acid (98 atom% $^2H_2$, Isotec, Miamisburg, OH) at a rate of 0.04 μmol/kg/min. Another catheter was placed in a contralateral dorsal hand vein, which was heated to obtain arterialized blood samples. Samples were taken before infusion of tracer and during isotopic steady state at 70, 80, and 90 minutes of isotope infusion.

Plasma fatty acids were prepared from 200 μL plasma by addition of 200 μL buffer (0.2 mol/L potassium phosphate and 0.05 mol/L tetrabutylammonium hydrogen sulfate, pH 9.0) and 200 μL iodomethane (5% vol/vol in dichloromethane). After vortexing the mixture at room temperature for 15 minutes, lipids were extracted with 3 mL hexane and dried under vacuum. The lipids were redissolved in a small volume of hexane, passed onto a SPE cartridge (LC-Si SPE tubes, 3-mL size; Supelco, Bellefonte, PA), and washed with 2 column volumes of hexane. Fatty acid methyl esters were eluted with 2% ethyl acetate in hexane, dried under vacuum, dissolved in 100 μL heptane, and transferred to autosampler vials for GC/MS analysis. Enrichment of methyl palmitate was measured by GC/MS on a Hewlett-Packard (Palo Alto, CA) 5971A MSD equipped with a 30-m × 0.32-mm Omegawax 250 capillary column (Supelco). Ions were formed by electron impact ionization, and molecular ions at *m/z* 270 (m + 0) and 272 (m + 2) were selectively monitored.[5] Palmitate in biological samples was completely resolved from nearby components, thus allowing baseline-to-baseline peak area integrations to be performed. The rate of appearance (Ra) of palmitate in plasma was calculated by dividing the tracer infusion rate by the TTR during isotopic plateau.[3]

$^{15}N_2$-Urea

A 62-year-old male was placed on a low-protein liquid formula diet containing 0.5 g protein/kg/d and 35 kcal/kg/d (Ensure; Ross Laboratories, Columbus, OH) for 3 days. On the fourth day, the liquid formula was divided into equal aliquots and given every 30 minutes from 6 AM to 4 PM. A primed (83.6 μmol/kg) continuous infusion (0.15 μmol/kg · min) of $^{15}N_2$-urea (99 atom% ^{15}N; Cambridge Isotope Laboratories, Andover, MA) was infused for 8 hours from 8 AM to 4 PM. Arterialized plasma samples were obtained from a heated hand vein prior to tracer administration and at 30, 60, 90, 120, 150, 180, 240, 300, 360, 420, 440, 460, and 480 minutes of tracer infusion. Urea was recovered by cation-exchange chromatography and converted to the *tert*-butyldimethylsilyl (tBDMS) derivative as previously described.[15,16] Samples and isotopic enrichment standards were analyzed by EI ionization GC/MS on a Hewlett-Packard 5971A MSD with a 30-m × 0.25-mm DB-17 capillary column (J & W Scientific, Folsom, CA) using the *m/z* 231 (m + 0) and 233 (m + 2) ions, which correspond to the unlabeled and labeled ions, respectively, after loss of *tert*-butyl.[15] Urea in biological samples was completely resolved from nearby components, thus allowing baseline-to-baseline peak area integration to be performed.

^{13}C-Leucine

A 16-year-old male was studied after a 10-hour fast using an 8-hour primed (0.85 mg/kg) continuous (0.85 mg/kg/h) infusion of L-1-^{13}C-leucine (99 atom% ^{13}C; MSD Isotopes, Montreal, Canada).[17] Plasma samples were obtained before tracer infusion, at frequent intervals during tracer infusion, and for 4 days after stopping the tracer infusion (a total of 30 samples). Plasma amino acids were isolated from 0.3 mL deproteinized plasma by cation-exchange chromatography, derivatized to *N*-heptafluorobutyryl-*n*-propyl (HFB propyl) esters,[17,18] and dissolved in ethyl acetate. Leucine enrichment was determined by GC/MS on a Hewlett-Packard 5988 system equipped with a 30-m × 0.25-mm DB-17 capillary column using 1-μL injections. Ions were formed by methane negative chemical ionization (NCI) and were selectively monitored at *m/z* 349 (m + 0) and 350 (m + 1), which correspond to the unlabeled and labeled ions, respectively, after loss of HF. Samples were also analyzed by EI ionization GC/MS on a Hewlett-Packard 5971A MSD with a 30-m × 0.25-mm DB-17 capillary column using the *m/z* 313 (m + 0) and 314 (m + 1) ions, which correspond to the unlabeled and labeled ions, respectively, after loss of the side chain from the molecular ion. Each sample was analyzed with two volumes injected (1 and 2 μL) for the EI application. Leucine in biological samples was completely resolved from nearby components for both GC/MS applications, thus allowing baseline-to-baseline peak area integration to be performed.

Preparation of Isotopic Enrichment Standards

Stock solutions were prepared for each pure isotopic tracer ($^2H_2$-palmitate, $^{15}N_2$-urea, and ^{13}C-leucine) and each corresponding unlabeled tracee to known weight percent compositions. Tracer and tracee solutions were mixed gravimetrically to obtain final solutions containing TTRs that spanned the range of enrichments encountered in *in vivo* tracer infusion studies (typically 0% to 10%). Aliquots of enrichment standards were dried and derivatized in the same manner as the biological samples. Stock solutions of methyl palmitate (~1 mmol/L) and HFB propyl leucine enrichment standards (~0.1 mmol/L) were stable and used repeatedly over a period of several months. Enrichment standards for tBDMS-urea were freshly prepared for each set of biological samples.

Determination of TTR

The TTR was measured by two conventional methods and our novel approach. Method 1, the R-R_0 approach, calculated the TTR directly from measured ion abundance ratios by the relationship TTR = R − R_0,[3] where R and R_0 represent the measured tracer to tracee ion abundance ratios for enriched and unenriched (preinfusion) samples, respectively. Method 2, the linear standard curve approach, involves a linear standard curve where the measured R is regressed against the known TTR of a series of isotopic enrichment standards containing a range of peak areas that span those of the biological samples. Typical quantities of standards analyzed were 0.1 to 1 nmol on the column for EI and 0.01 to 0.1 nmol for NCI applications. The development of method 3, our new approach that incorporates concentration dependencies into the standard curve approach, is described in the Results.

RESULTS

$^2H_2$-Palmitate

Measurement of the plasma palmitate TTR in plasma samples is shown in Table 1. Runs 1 and 2 represent independent

Table 1. Reproducibility of Methods Used to Calculate the TTR and Ra of Palmitate

Method for TTR Determination	Measured TTR in Plasma Samples (min of $^2H_2$-palmitate infusion)								Calculated Palmitate Ra (μmol/kg/min)
	70 min		80 min		90 min		Overall		
	Mean	CV	Mean	CV	Mean	CV	Mean	CV	
$R-R_0$									
Run 1	0.0198	8.6%	0.0179	6.1%	0.0185	5.4%	0.0187	7.5%	2.14
Run 2	0.0285	9.8%	0.0254	2.0%	0.0273	10.6%	0.0271	8.9%	1.48
Linear standard curve									
Run 1	0.0284	8.5%	0.0258	5.8%	0.0265	5.3%	0.0269	7.4%	1.49
Run 2	0.0320	9.4%	0.0287	1.7%	0.0307	10.1%	0.0305	8.5%	1.31
Current approach									
Run 1	0.0324	2.8%	0.0297	2.4%	0.0304	1.3%	0.0308	4.5%	1.30
Run 2	0.0321	2.8%	0.0302	1.3%	0.0305	0.6%	0.0309	3.6%	1.29

NOTE. TTR values are the mean and CV of 3 measurements made after injecting 0.5, 1.0, and 1.5 μL of each sample. Runs 1 and 2 represent analyses of the same samples separated by several weeks.

measurements of the same sample vials analyzed on two occasions several weeks apart. Each run included analyses of three separate sample injections spanning a threefold range in sample quantity injected (0.5, 1.0, and 1.5 μL).

When the TTR was determined directly from measured ion abundance ratios using the $R - R_0$ mathematical model, there was a large day-to-day variability. TTR values from run 2 (overall TTR, 0.0271) were 45% higher than those obtained from run 1 (overall TTR, 0.0187). This large difference in the TTR translated into a 31% difference in the calculated palmitate Ra (2.14 and 1.48 μmol/kg/min for runs 1 and 2, respectively). The background R_0 m + 2/m + 0 ion abundance ratio was the same in the two analyses (0.0228 ± 0.0012 and 0.0220 ± 0.0021 for runs 1 and 2, respectively). Therefore, a substantial difference in measurement accuracy between the two runs was not evident from the preinfusion samples. In addition to the day-to-day variability, there was a substantial variability resulting from concentration dependency, as the coefficient of variation (CV) using three volumes (0.5, 1.0, and 1.5 μL) was 5% to 10% for individual samples.

Conventional standard curves for $^2H_2$-palmitate were linear for both analyses (Fig 1), but revealed a markedly different response of measured ion abundance ratios during different runs (slope of measured m + 2/m + 0 ratio *v* true TTR was 0.6316 and 0.9258 for runs 1 and 2, respectively). Determination of the TTR from runs 1 and 2 using the linear standard curve (Table 1) resulted in closer agreement between the two analyses, but run 2 (overall TTR, 0.0305) was still 13% higher than run 1 (TTR, 0.0269), with a resulting 12% difference in the apparent Ra (1.49 *v* 1.31 μmol/kg/min for runs 1 and 2, respectively). For 14 standard curves of $^2H_2$-palmitate enrichment standards run over several months, the mean slope was 0.993 with a CV of 13.8%. The slopes ranged from 0.632 to 1.163 (84% range from lowest to highest value). There was also considerable variability in the intercepts of these standard curves (mean, 0.0222; CV, 9.8%), with no apparent correlation between the slope and intercept values (R^2 = .091).

The conventional linear standard curve did not decrease variability in the TTR when different volumes of sample were analyzed (Fig 1). This concentration dependency for enrichment standards from run 1 is detailed in Fig 2. The measured

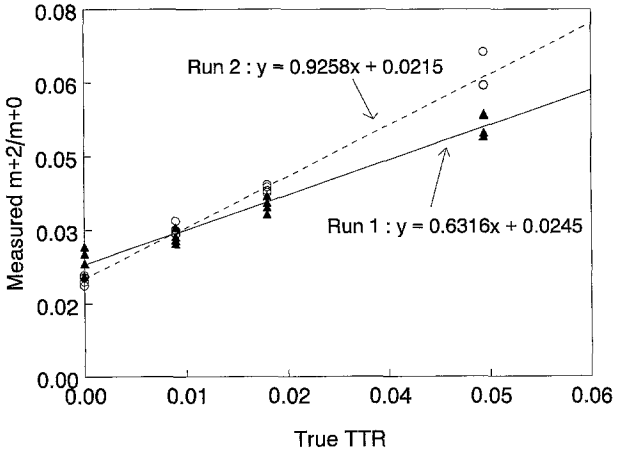

Fig 1. Conventional linear standard curve for $^2H_2$-palmitate. Samples of known TTR enrichment were analyzed during runs 1 and 2 (Table 1). The measured m + 2/m + 0 ion abundance ratio is plotted against the true TTR. Each standard was measured 4 times using volumes of 0.5, 1.0, 1.5, and 2.0 μL.

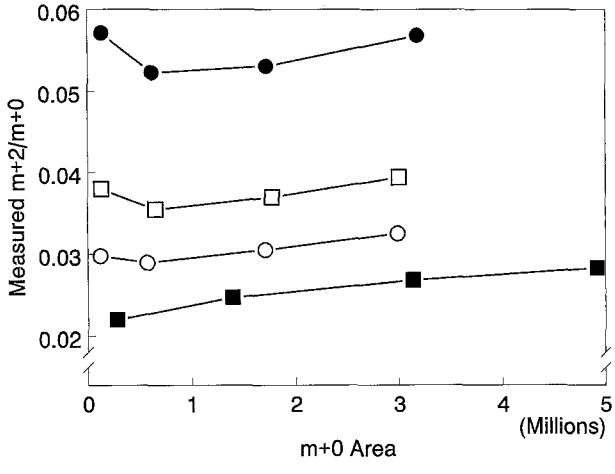

Fig 2. Effect of varying the volume of injected sample on the measured ion abundance ratio for isotopic enrichment standards. Four different volumes of $^2H_2$-palmitate standards of known enrichment were analyzed (0.5, 1.0, 1.5, and 2.0 μL). Results shown are the measured m + 2/m + 0 ion abundance ratios as a function of observed m + 0 peak area. ■, TTR = 0; ○, TTR = 0.011; □, TTR = 0.022; ●, TTR = 0.047.

m + 2/m + 0 ratio increased with increasing peak area at large m + 0 peak areas for all levels of enrichment. However, as peak areas became smaller, these curves were erratic, with measured ratios decreasing for the natural abundance standard (TTR = 0) and increasing to a variable extent for each enriched standard. Anomalies associated with small peak areas are more likely due to peak tailing and deviations in integrator performance rather than insufficient signal strength, since even the smallest peaks achieved a signal to noise ratio greater than 50:1 for m + 2 natural abundance. There was no region of m + 0 peak area over which the measured m + 2/m + 0 ratio was constant for any level of enrichment. There was a marked day-to-day variation in the exact shape of these curves; however, the tendency for measured ratios to increase with larger peak areas and to be erratically elevated or decreased at smaller peak areas was a universal pattern for $^2H_2$-palmitate. It did not seem feasible to develop a mathematical model to accommodate concentration dependencies into the standard curve approach when the data were viewed in the format of measured ion abundance ratios against the m + 0 peak area (hereafter referred to as a ratio *v* area plot), due to the erratic nature of these plots near the origin.

Our new approach that accommodates concentration dependencies into the standard curve analysis by correlating the observed m + 2 peak areas directly against the observed m + 0 areas (hereafter referred to as an area *v* area plot) is shown in Fig 3. It was necessary to use a second-order regression rather than a first-order to achieve an optimal fit to the area versus area data as we previously demonstrated.[5] For the $^2H_2$-palmitate data

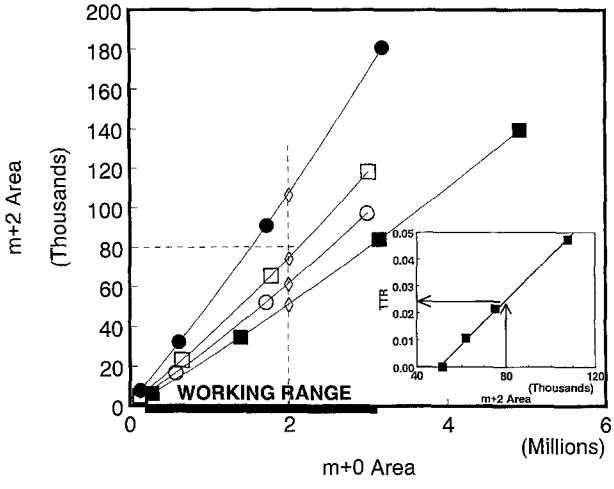

Fig 3. General procedure for incorporating concentration effects into a standard curve. Each standard of $^2H_2$-palmitate of known TTR was run with 0.5, 1.0, 1.5, and 2.0 μL sample analyzed. The data illustrated are the same results as in Fig 2. The observed m + 2 peak areas were directly correlated against the observed m + 0 peak areas using a second-order regression. To determine the TTR of an unknown sample, the respective m + 2 peak areas that each standard would have produced for the same m + 0 peak area obtained for that sample are determined (◇), and the sample TTR is determined by constructing a secondary regression (linear) relating the m + 2 peak areas to the true TTR (inset). ■, TTR = 0; ○, TTR = 0.011; □, TTR = 0.022; ●, TTR = 0.047.

illustrated, the following regression lines were obtained:

$$\text{TTR} = 0: \quad (m+2) = 8.3\text{E-}10(m+0)^2 + 0.0245(m+0) - 899, \quad R^2 > .9999$$

$$\text{TTR} = 0.011: \quad (m+2) = 1.6\text{E-}09(m+0)^2 + 0.0276(m+0) + 242, \quad R^2 > .9999$$

$$\text{TTR} = 0.022: \quad (m+2) = 2.1\text{E-}09(m+0)^2 + 0.0330(m+0) + 653, \quad R^2 > .9999$$

$$\text{TTR} = 0.047: \quad (m+2) = 2.8\text{E-}09(m+0)^2 + 0.0476(m+0) + 1{,}475, \quad R^2 > .9999$$

In each case, the second-order coefficients were highly significant ($P < 10^{-6}$). These area versus area regressions provide a simple mathematical model that explains the erratic behavior of the ion abundance ratio plot (Fig 2) as due to the summation of two effects. First, it is noted that the intercept of the area versus area plot was negative for the natural abundance sample and increased with increasing enrichment. The magnitude of these intercepts is imperceptible in comparison to the scale of the area versus area plot (Fig 3), but nevertheless, these nonzero intercepts account for the erratic behavior of the ratio versus area plots at smaller peak areas (Fig 2). Thus, the measured m + 2/m + 0 ratio of the natural abundance standard decreases as peak areas approach zero (Fig 2) because the area versus area plot has a negative intercept (Fig 3 and the regression coefficients already presented), whereas the increased ratios as peak areas approach zero for the other standards (Fig 2) are due to the increasing intercepts in the area versus area plots (Fig 3 and the regression coefficients). This effect dominating at small peak areas is likely due to errors associated with integrating smaller peaks (peak tailing, baseline identification, detection threshold, etc.). The second effect, the second-order nonlinearity, dominates at larger peak areas and is likely due to true concentration-dependent effects within the instrument. This second-order nonlinearity causes the m + 2/m + 0 ion abundance ratios to increase at larger peak areas (Fig 2); if the left and right side of the regression equations are divided by (m + 0), it is evident that the (m + 2)/(m + 0) ratio is dependent on the (m + 0) area.

Development of New Approach

An example illustrating the use of our novel approach to incorporate concentration dependencies into the standard curve approach is illustrated in Fig 3. Suppose that the m + 0 and m + 2 peak areas of an unknown sample measure 2,000,000 and 80,000, respectively. The first step is to determine the m + 2 peak areas that each enrichment standard would have produced if they had the same m + 0 area as the sample; this is achieved using the regression coefficients already outlined. Next, a secondary regression (Fig 3, inset) is constructed to correlate the true TTRs against these predicted m + 2 areas (TTR = 0.024 for the present example). It has been our experience that the secondary plot is linear, although some conditions (eg, coverage of a wide range of enrichments) could require a nonlinear regression. A valid working range for observed m + 0 peak

areas can be established by inspection of the area versus area plot (Fig 3), such that no samples will be evaluated if their observed m + 0 peak areas are so small or large to require unwarranted extrapolations beyond the standards. It should be emphasized that it is necessary to run the set of concentration-dependent standards in time series with the biological samples being analyzed, since tuning and conditions within the ionization source can drift over time.

TTR values obtained by our new approach are compared with those obtained using the $R - R_0$ and linear standard curve approaches in Table 1. Results from runs 1 and 2 were virtually identical following this procedure to apply concentration corrections for each of the individual time points and for the overall mean values, resulting in virtually identical calculated palmitate Ra values. Furthermore, there was a dramatic reduction in the standard deviation for replicates using different volumes of sample compared with either the $R - R_0$ or linear standard curve approaches, which do not account for concentration dependency. In this example, the corrected palmitate Ra was considerably lower than the Ra obtained directly from measured ion abundance ratios using the $R - R_0$ approach for either of the two runs.

$^{15}N_2$-Urea

Application of our new approach for plasma $^{15}N_2$-urea enrichment is illustrated in Fig 4. Using the $R - R_0$ approach, there was greater than a 10% range in the apparent TTR at every time point over a threefold range of sample volume injected into the instrument (0.5, 1.0, and 1.5 μL). However, our new approach virtually eliminated this concentration-dependent variability. Linear standard curves for the tBDMS derivative of $^{15}N_2$-urea were less variable than for $^2H_2$-palmitate. For 13 standard curves run over several months, the mean slope was 0.976 (CV, 6.2%) with a range of 0.914 to 1.151 (26% range from lowest to highest slope).

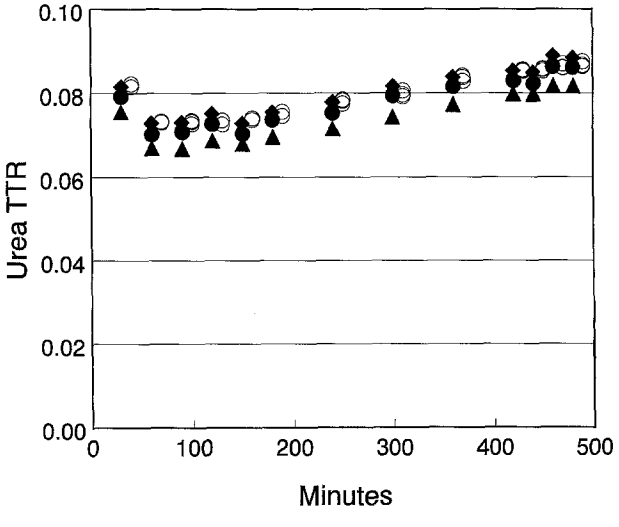

Fig 4. Enrichment of plasma urea during a primed constant infusion of $^{15}N_2$-urea. Samples were analyzed using 3 volumes (0.5, 1.0, and 1.5 μL). Results are shown for 3 volumes injected using the $R - R_0$ approach (▲, 0.5 μL; ●, 1.0 μL; ◆, 1.5 μL) and for all 3 volumes using the new approach that corrects for concentration effects (○; time values for all 3 volumes injected are offset for clarity).

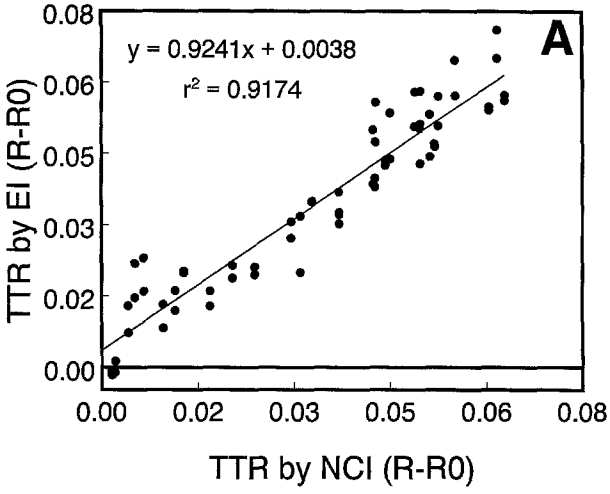

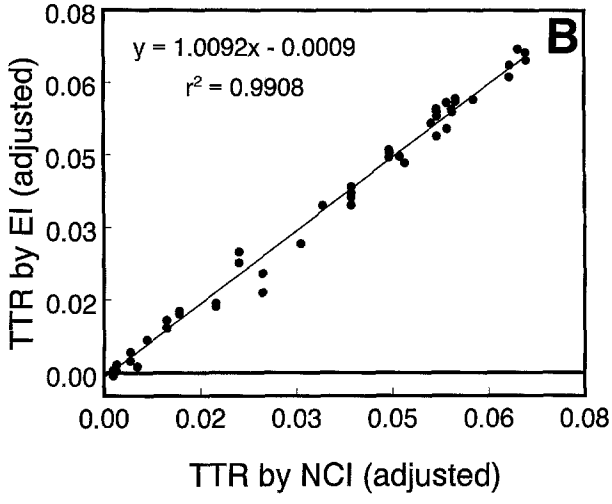

Fig 5. Correlation of 1-^{13}C-leucine enrichment by EI ionization GC/MS versus NCI GC/MS. Plasma amino acids were recovered from various time points during and after an 8-hour primed constant infusion of 1-^{13}C-leucine. Enrichments of HFB propyl ester derivatives were measured by either EI or NCI GC/MS. (A) TTR from EI and NCI analyses determined using the $R - R_0$ approach. (B) TTR from EI and NCI analyses adjusted using the new concentration-dependent standard curve approach.

^{13}C-Leucine

Figure 5 illustrates the use of our approach to measure enrichment of plasma leucine during an infusion of 1-^{13}C-leucine. Each sample was analyzed once by NCI and in duplicate by EI GC/MS. EI and NCI results differed when the TTR was calculated directly from ion abundance ratios using the $R - R_0$ approach: the regression of EI against NCI values had a slope of 0.92, was offset from the origin, and exhibited considerable variability ($R^2 < .92$, standard error = 0.0062). Most of the variability between methods was due to concentration dependency, particularly in the EI measurements, due to a 50-fold range in measured m + 0 peak areas resulting from dual volumes injected (1 and 2 μL) and variable sample recovery for samples analyzed. Concordance between the data sets was dramatically improved (slope of unity, intercept not signifi-

cantly different from zero, $R^2 > .99$, standard error = 0.0024) when the results were adjusted using our approach.

DISCUSSION

In this report, we present a new approach for determining isotopic enrichment by GC/MS that improves the accuracy and precision of TTR measurements. In contrast to previous approaches that either determine TTR directly from observed ion abundance ratios ($R - R_0$) or use a simple linear standard curve, our approach incorporates nonlinear concentration effects within a standard curve. The approach is implemented by analyzing each isotopic enrichment standard over a range of measured GC/MS peak areas that span those obtained for the biological samples being analyzed. Our results demonstrate that this approach is useful for analyzing many of the substrates (fatty acids, urea, and amino acids) and tracers (^2H, ^{15}N, and ^{13}C) commonly used in studying intermediary metabolism in vivo by decreasing the variability caused by concentration dependency and day-to-day instrument response.

We have noted a marked day-to-day variability in instrument response for the applications evaluated, as well as other GC/MS applications not included in this report. The magnitude of day-to-day variability differs between applications and tends to be more variable for applications that are more sensitive to concentration effects. For example, the methyl palmitate and tBDMS-urea applications exhibit considerable concentration dependency and day-to-day responses (slopes of linear standard curves had a low to high range of 84% and 26%, respectively). Most other applications that we routinely use exhibit less concentration dependency and also have less variable day-to-day standard curve slope responses, such as the tBDMS derivative of 5,5,5-[$^2H_3$]-leucine by EI (range of slopes, 10%), the HFB derivative of 6,6-$^2H_2$-glucose by EI (range, 13%), the HFB derivative of 1,1,2,3,3-[$^2H_5$]-glycerol by EI (range, 7%), and the HFB derivative of 2-^{13}C-glycerol by either EI (range, 14%) or NCI (range, 5%) (data not shown). The HFB derivative of 1,1,2,3,3-[$^2H_5$]-glycerol by NCI[19] exhibits the greatest anomalies of any application tested (data not shown): measured ion abundance ratios can vary twofold over a fivefold range of sample quantity, and the mean slope of the linear standard curve was 1.48 (CV, 21%) with a range of 1.13 to 2.44 (115% range from lowest to highest) for 18 standard curves. The mechanisms responsible for the extreme variability of the HFB-$^2H_5$-glycerol response by NCI compared with the extremely good reproducibility of HFB-^{13}C-glycerol are currently being investigated.

Much of the day-to-day variability in instrument response is due to variable tuning conditions, especially when using the autotune feature of the Hewlett-Packard MSD system. The autotune feature is designed to provide nominal instrument performance by adjusting the absolute and relative intensities for selected fragments of the tuning compound (typically, ion fragments at *m/z* 69, 219, and 502 of perfluorotributylamine), nominal quadrupole peak resolution, and nominal mass axis calibration. Unfortunately, the manufacturer-set limits for these parameters are broad such that the autotune does not provide the reproducibility desired for precise isotope enrichment measurements. Substantially different ion ratio measurements can result on repeating an autotune. By comparison, once a given tuning condition is established, the drift of instrument performance over a period of days is relatively minor. Therefore, we advocate using autotune infrequently (eg, after cleaning the source) just to provide nominal instrument performance, with minor daily manual adjustments to the mass axis calibration and spectral peak width resolution to improve ion ratio measurement precision.

In addition to differential variability in the day-to-day response of linear standard curves, applications also differ in their sensitivity to concentration dependency. For example, methyl palmitate undergoes protonation (self-chemical ionization) in the EI ionization source as neutral molecules are charged to form ions with masses 1 dalton greater in a concentration-dependent manner.[5] Methyl esters are particularly prone to undergo self-chemical ionization. We do not observe as high a degree of concentration dependency for other applications as we do for methyl palmitate; for example, the tBDMS derivative of palmitate exhibits considerably less concentration dependency on the same GC/MS system (B.W. Patterson, unpublished observations). It would be preferable to avoid derivatives that are sensitive to self-chemical ionization whenever possible. Unfortunately, in the case of palmitate, virtually all studies have used the methyl ester for analysis since the first report using stable isotopically labeled palmitate appeared.[20] The present report provides a solution to improve the reliability of GC/MS measurements for such applications.

Not all applications undergo self-chemical ionization as does methyl palmitate. However, limitations in instrument design will produce concentration-dependent nonlinearities from sources such as ion-molecule collisions, charge effects, detector nonlinearities, etc., in the absence of self-chemical ionization. We have observed that the magnitude of these effects may vary from one day to another (eg, as tuning conditions and source cleanliness vary) and from one instrument to another for the same application (ie, variations in instrument design, particularly the quality of vacuum). Our algorithm corrects for multiple sources of nonlinearity simultaneously, whether due to self-chemical ionization or limitations in instrument design.

We speculate that different applications may vary in their sensitivity to processes that bias measured ion abundances, such as charge effects or self-chemical ionization. These processes are in turn likely to be sensitive to day-to-day variability in tuning conditions and/or cleanliness of the ionization chamber of the mass spectrometer. It is not possible to control all sources of variability within the ion source, so day-to-day variability in instrument conditions could result in variable concentration effects. Applications that are particularly sensitive to concentration dependencies appear to exhibit greater variability in day-to-day instrument response, as exhibited by variable standard curve slopes. Our new approach is unique in its ability to correct for concentration effects, as well as day-to-day variability in instrument response, based on the concentration dependencies of enrichment standards measured under concurrent GC/MS instrument conditions. However, some applications are not amenable to our approach because a standard curve cannot be applied, such as when multiple overlapping tracers are measured simultaneously (eg, simultaneous measurement of 1-^{13}C- and $^2H_3$-leucine) or when the product being measured is a conversion product of the infused tracer (eg, mass isotopomer distribution applications such as ^{13}C-acetate incorporation into

plamitate, or when measuring the enrichment of $^2H_3$-α-ketoisocaproate following an infusion of $^2H_3$-leucine unless $^2H_3$-α-ketoisocaproate is available as a GC/MS enrichment standard).

Although in the present study we demonstrate our new approach using three examples consisting of single sets of data, virtually all GC/MS applications that we use to evaluate metabolic substrate kinetics exhibit some degree of concentration dependency. This concentration dependency may be manifested in two ways: nonlinearity of the area versus area plot and/or a nonzero intercept for these plots (Fig 3). The former effect dominates with large quantities of sample injected (eg, >0.5 nmol by EI), whereas the latter effect dominates with small quantities injected (eg, <0.2 nmol). Nonlinearities can result from numerous processes, such as self-chemical ionization, dispersions from charge effects, and detector nonlinearity. The magnitude of the second-order coefficient tends to increase with increasing enrichments. Nonzero intercepts for the area versus area plots may result from baseline integration errors, spectral overlap of adjacent ions (especially in low-resolution quadrupole mass spectrometers), and poor instrument sensitivity (low signal to noise ratios). These intercepts tend to increase with increasing isotopic enrichment.

The concentration dependency of measured ion abundance ratios can be minimized by maintaining constant peak areas of isotopic enrichment standards and samples. However, this often requires varying the amount of sample delivered to the GC column, which is impractical when an autosampler is used to inject samples. Variations in sample recovery during processing and derivatization and physiological alterations in metabolite concentration during a tracer infusion protocol can generate a wide range of metabolite concentrations. An initial "pre-run" could be performed to determine relative sample concentrations, and a second run performed after adding appropriate volumes of solvent to each vial to normalize sample concentrations. However, it can still be difficult to control peak areas within a factor of two using this approach because of the volatility of many solvents. Moreover, we have observed significant concentration dependencies even over a twofold range of concentrations for some applications (eg, methyl palmitate in EI). In addition, a "pre-run" wastes valuable sample volume and instrument time. Our approach establishes a valid working range for a given analysis based on an area versus area graphical format (Fig 3); this working range may include peak areas that were previously considered too small or too large to provide reliable results. Analyzing each isotopic enrichment standard with four or more different volumes and injecting each study sample with at least two volumes (large and small) helps to ensure that at least one of the volumes injected for each sample will be within the valid working range (Fig 3).

In conclusion, we have demonstrated that an approach incorporating concentration dependencies into a standard curve analysis increases the accuracy of GC/MS enrichment measurements by accounting for both instrument response and concentration-dependent effects. The improvement in accuracy results in improved precision. The approach is generically applicable to any GC/MS application amenable to analysis by a standard curve.

ACKNOWLEDGMENT

We wish to thank Drs Gustav Schonfeld and Mickey Latour for the use of plasma samples obtained from a subject infused with 1-^{13}C-leucine.

REFERENCES

1. Hachey DL, Blais J-C, Klein PD: High precision isotopic ratio analysis of volatile metal chelates. Anal Chem 52:1131-1135, 1980

2. Cobelli C, Toffolo G, Foster DM: Tracer-to-tracee ratio for analysis of stable isotope tracer data: Link with radioactive kinetic formalism. Am J Physiol 262:E968-E975, 1992

3. Wolfe RR: Radioactive and Stable Isotope Tracers in Biomedicine: Principles and Practice of Kinetic Analysis. New York, NY, Wiley-Liss, 1992

4. Rosenblatt J, Chinkes D, Wolfe M, et al: Stable isotope tracer analysis by GC-MS, including quantification of isotopomer effects. Am J Physiol 263:E584-E596, 1992

5. Patterson BW, Wolfe RR: Concentration dependence of methyl palmitate isotope ratios by electron impact ionization gas chromatography/mass spectrometry. Biol Mass Spectrom 22:481-486, 1993

6. Derrick PJ: Isotope effects in fragmentation. Mass Spectrom Rev 2:285-298, 1983

7. Schoeller DA: Model for determining the influence of instrumental variations on the long-term precision of isotope dilution analyses. Biomed Mass Spectrom 7:457-463, 1980

8. Low IA, Liu RH, Barker SA, et al: Selected ion monitoring mass spectrometry: Parameters affecting quantitative determination. Biomed Mass Spectrom 12:633-637, 1985

9. Hu B, Qiu B: The nonlinearity of upper limiting pressure for quadrupole mass spectrometers. J Vac Sci Technol 5:2657-2660, 1987

10. Loveridge WD: Measurement of biases in the electron multiplier ion detection system of a Finnigan-MAT model 261 mass spectrometer. Int J Mass Spectrom Ion Proc 74:197-206, 1986

11. Matthews DE, Hayes JM: Systematic errors in gas chromatography–mass spectrometry isotope ratio measurements. Anal Chem 48: 1375-1382, 1976

12. Millard BJ: Quantitative Mass Spectrometry. London, UK, Heyden, 1978

13. Bush ED, Trager WF: Analysis of linear approaches to quantitative stable isotope methodology in mass spectrometry. Biomed Mass Spectrom 8:211-218, 1981

14. Yap WT, Schaffer R, Hertz HS, et al: On the difference between using linear and non-linear models in bracketing procedures in isotope dilution mass spectrometry. Biomed Mass Spectrom 10:262-264, 1983

15. Patterson BW, Carraro F, Wolfe RR: Measurement of ^{15}N enrichment in multiple amino acids and urea in a single analysis by gas chromatography/mass spectrometry. Biol Mass Spectrom 22:518-523, 1993

16. Patterson BW, Carraro F, Klein S, et al: Quantification of incorporation of [^{15}N]ammonia into plasma amino acids and urea. Am J Physiol 269:E508-E515, E515, 1995

17. Latour MA, Patterson BW, Pulai J, et al: The metabolism of apolipoprotein B-100 in a kindred with familial hypobetalipoproteinemia without a truncated form of apoB. J Lipid Res 38:592-599, 599, 1997

18. Patterson BW, Hachey DL, Cook GL, et al: Incorporation of a stable isotopically labeled amino acid into multiple human apolipoproteins. J Lipid Res 32:1063-1072, 1072, 1991

19. Matthews DE, Pesola GR, Kvetan V: Glycerol metabolism in humans: Validation of ^{2}H- and ^{13}C-labelled tracers. Acta Diabetol 28:179-184, 1991

20. Wolfe RR, Evans JE, Mullany CJ, et al: Measurement of plasma free fatty acid turnover and oxidation using palmitic acid. Biomed Mass Spectrum 7:168-171, 1980